*Remote Sensing for a Changing Europe*
*D. Maktav (Ed.)*
*IOS Press, 2009*


*doi:10.3233/978-1-58603-986-8-125*

# Evaluation of data fusion methods for agricultural monitoring based on synthetic images

A. S. Rodrigues, A. R. S. Marçal & M. Cunha
*Centro de Investigação em Ciências Geo-Espaciais, Faculdade de Ciências, Universidade do Porto, Portugal*

Keywords: synthetic images, data fusion, NDVI, agricultural monitoring.

ABSTRACT: There are several data fusion methods widely used to produce a high resolution multi-spectral image from a pair of images - a panchromatic high resolution and a multi-spectral lower resolution image. Although the fused images can be visually satisfactory, it is not clear whether they provide additional information for quantitative measurements made from satellite images. A methodology to evaluate data fusion algorithms is proposed, based on the production of synthetic images that reproduce real satellite images. An experiment was conducted testing the performance of six data fusion methods in the production of NDVI values for land parcels from SPOT HRG and Landsat TM data. The fusion methods evaluated were: Brovey, IHS Hexcone, IHS Cylinder, PCA, Wavelet IHS and Wavelet Single Band. The best data fusion method overall was found to be Wavelet IHS, although better results were obtained by using directly the lower resolution multi-spectral data instead. The software tools developed and a number of test images datasets are freely available at the SITEF website (www.fc.up.pt/sitef).

## 1 INTRODUCTION

The number of satellite sensors acquiring high and very high resolution images of the Earth has been steady increasing in the last few years. Most of these sensors use two complementary image modes – a multi-spectral image (M) and a higher spatial resolution panchromatic image (P). Examples of such sensors include IKONOS (multi-spectral image with 4m pixel and panchromatic image with 1m pixel), QuickBird (2.4m / 0.6m) and SPOT (10m / 5m, or 20m / 10m). The objective of data fusion in this context is to generate a multi-spectral image with both high spatial and spectral resolutions (Ranchin & Wald 2000). The effective application of a data fusion algorithm produces a high resolution multi-spectral (fused) image that is usually satisfactory for visual perception or cartographic applications. However, it is not clear whether the fused image provides valuable additional information when the aim is to make quantitative measurements from the satellite image.

The purpose of this work is to investigate if the use of data fusion improves the information provided by satellite images for quantitative measurements in a practical application (agriculture monitoring), and to evaluate the most widely used data fusion methods using synthetic images.

## 2 DATA FUSION

There are several well established image data fusion methods, such as Intensity Hue Saturation (IHS), Principal Components Analysis (PCA), Brovey and Wavelet (Wang *et al* 2005b).

One of the simplest methods is the Brovey fusion. The fused image is simply obtained by a normalization of M, which is then multiplied by P (Wehrmann *et al* 2005). In the IHS method, a RGB color composite produced from M is mapped to the IHS color space. The I component is then replaced by P, after histogram matching, and the resulting IHS image converted back to the RGB color space. There are three IHS models – cylinder, triangular and hexcone - providing slightly different results in the RGB colors produced. The IHS method is simple and effective, but it can only be applied to multi-spectral images with 3 bands. An alternative is to use the PCA method, which can be applied to images with any number of bands, and works in a somehow related way. Initially the principal components of M are computed. The first component (which has the most information) is replaced by P, after histogram matching, and then the principal components are converted back to the initial space (Wald 2002). The wavelet method is the most recent one and harder to implement. Four images are produced from P: one of rough detail and three of high resolution corresponding to the horizontal, vertical and diagonal components. The rough image of P is replaced by a histogram matched version of M, after which the inverse transform is computed to produce the final fused image (Balcik & Sertel 2007). The wavelet fusion can be used in one of three models: Single Band, IHS and PCA.

The quality of the fused image depends on the method used and on the data itself. The evaluation is usually based on visual analysis, or sometimes on statistics that examine the similarity or the discrepancies between the fused and original products, on a pixel by pixel and band by band basis. The quantitative evaluation of an image produced by data fusion is not a straight forward task, as there is usually no reference (high resolution multi-spectral image) to be used for comparison. The common approach is to degrade the fused image to the spatial resolution of M, and to compare it with M (Meenakshisundaram & Couloigner 2005). Several parameters have been used for this task, such as Euclidean Distance (Wang *et al* 2005a), Coefficient of Correlation (Scheunders & Backer 2001) and Root Mean of Square Error (Wehrmann *et al* 2005). All these evaluation parameters focus on the differences between individual pixels and bands. However, for many remote sensing applications the objective is to extract information based on a combination of bands for areas with several pixels. One common example is the production of Normalized Difference Vegetation Index (NDVI) values for land parcels (Jensen 2000).

The NDVI is computed using the reflectance values in the red ($\rho_R$) and near infrared ($\rho_{NIR}$) bands, using (1). Two NDVI ranges were used: -1 to 1 and 0 to 1, by setting to zero all negative values. The interval 0 to 1 was used as the standard range.

$$NDVI = \max\left\{0, \frac{\rho_{NIR} - \rho_R}{\rho_{NIR} + \rho_R}\right\} \tag{1}$$

The calibration of image band *i* to reflectance ($\rho_i$) is done using (2), where $R_i$ is the radiance, $E_{0i}$ the equivalent solar spectral irradiance and $\theta_s / \theta_v$ are the solar/viewing zenith angles (FIFE 2004). The radiance is obtained directly from the recorded Digital Numbers (DN) using a linear relation $R_i = \alpha_i DN + \beta_i$, where $\alpha_i$ and $\beta_i$ are the calibration coefficients (FIFE 2004, GAEL 2003).

$$\rho_i = \frac{\pi R_i}{E_{0i} \cos(\theta_s) \cos(\theta_v)} \tag{2}$$

A suitable evaluation of the quality of a data fused product would be to compare the value of NDVI computed using the data fused image ($NDVI_{FUS}$) with the NDVI obtained directly using a high resolution multi-spectral image ($NDVI_{MH}$). The absolute error in NDVI (δ) is thus computed from (3). However, this approach is difficult to implement using real satellite images, as there is usually no high resolution multi-spectral image available to use for validation of the fused image.

$$\delta = \left| NDVI_{MH} - NDVI_{FUS} \right| \tag{3}$$

## 3 METHOD

The data fusion evaluation was done using synthetic images produced with the Synthetic Image Testing Framework (SITEF).

### 3.1 *Synthetic Image Testing Framework (SITEF)*

The SITEF provides images with controlled spatial and spectral characteristics, which simulate real multi-spectral satellite images by making use of a reference image where training areas are identified (Marçal & Rodrigues 2008). The SITEF software is freely available at www.fc.up.pt/sitef, where some test images datasets are also available. The objective is to simulate land parcels of various sizes with different land cover types. Initially, the number of land cover types (c), the size of the smallest unit (u), the range of sizes (s) and a repetition parameter (r) are used to produce a base image. As an example, figure 1 shows four base images, all with u=4, s=4, r=2, and with c=4, 5, 6, 7. The smallest squares on the top left section of these images have 4 by 4 pixels, while the largest ones on the lower right have 16 by 16 pixels (s=4). In this case there are 4 parcels of each size (r=2). The whole images are 80 by 80 pixels, with a total of 64 parcels. There are 4 single unit parcels (4 by 4 pixels), and generally 4 parcels of i by j units, with i,j=1,2,3,4. The classes are assigned to parcels assuring that two neighboring parcels always belong to different land cover types.

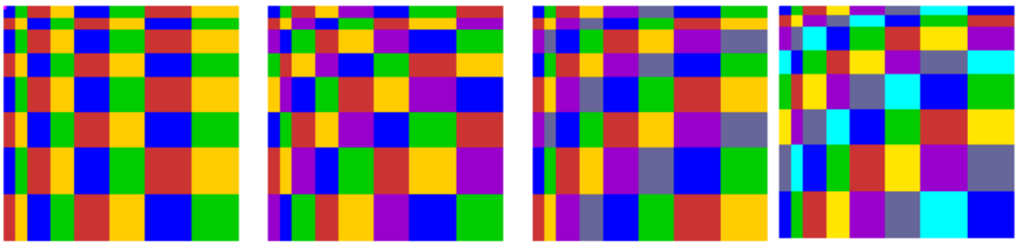

Figure 1. Synthetic base images with c=4, 5, 6, 7 (left to right), all with u=4, s=4, r=2.

The base image and a reference satellite image are used to produce a multi-spectral synthetic image. Reference areas are previously established in the multi-spectral satellite image, one for each land cover class considered (1, …, c). The multi-spectral synthetic image produced (MH) will have the same number of bands as the reference satellite image, with the pixel values of each class in the base image replaced by random vectors from the reference areas. A lower resolution version (ML) of this image is also produced (reduced in size by a factor of 2), as well as a high resolution panchromatic image (PAN). The process is presented schematically in figure 2.

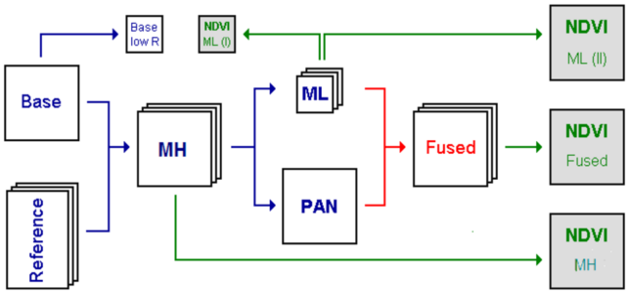


Figure 2. Schematic representation of the data fusion evaluation experiment: MH - multi-spectral high resolution, ML - multi-spectral low resolution and PAN - panchromatic high resolution.

### 3.2 *Test images*

Two satellite images, from Landsat and SPOT, both covering a mountainous area around Montalegre (Portugal) were used as reference. The SPOT 5 HRG image was acquired in 2005 and the Landsat 5 TM image in 1997. Two test images were produced using the SPOT (TIS) and Landsat (TIL) satellite images as reference. A total of six land cover classes were considered: irrigated (1) and non-irrigated permanent semi-natural mountain meadows (2), evergreen forest (3), deciduous forest (4), communitarian pastures (5) and annual crops (6).

The multi-spectral synthetic images TIS and TIL were created with u=3, s=8, r=5 and c=6, corresponding to an image size of 540 by 540 pixels. Although both SPOT HRG and Landsat TM sensors provide multi-spectral images with more than three bands, the synthetic images were both produced with three bands, as only the red and near infrared bands are used to compute the NDVI and the spectral coverage of the images only overlap three bands. Three versions were prepared for each test image: MH - multi-spectral high resolution, ML - multi-spectral low resolution and PAN - panchromatic high resolution. The MH synthetic images are presented in figure 3, with histogram linear enhancement. The lower resolution multi-spectral images were created by averaging every 2 by 2 pixel block into a single pixel. The panchromatic versions were created by combining the three bands with weights that reproduce the spectral response of the satellite sensors. For SPOT 5 HRG these weights are 0.617, 0.383, 0.000 for bands 1,2,3. As Landsat 5 TM does not have a panchromatic band, the characteristics of ETM panchromatic band were used instead. The relative contributions from Landsat 5 TM bands 2,3,4 to reproduce the ETM panchromatic band are: 0.333, 0.335, 0.332. Alternative versions of the test images used here are available at SITEF (www.fc.up.pt/sitef) with 8 and 5 classes – the Montalegre dataset.

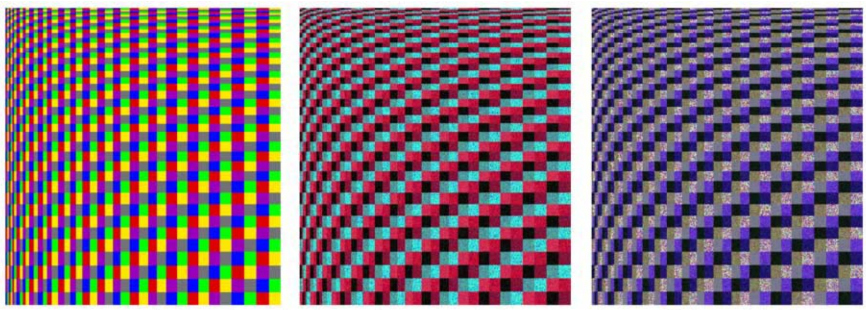

Figure 3.Base image (left) and synthetic test images TIS (center) and TIL (right), with histogram linear enhancement.

An evaluation of the spatial resolution degradation process was also made. A Gaussian filter of size 19 and standard deviation 5 was applied to the SPOT MH image, resulting in an image without high frequencies (MHGauss). From the MHGauss image two versions were created: MLGauss and PANGauss.

## 4 RESULTS

The data fusion experiment was performed using PCIGeomatica (PCI Geomatics 2005) and ERDAS Imagine (Erdas Imagine 2007) software. The versions ML and PAN of the test images were used as input for the data fusion methods tested, resulting in six fused images: (1) Brovey, (2) PCA, (3) IHS model Cylinder, (4) IHS model Hexcone, (5) Wavelet model IHS and (6) Wavelet model Single Band.

A total of nine NDVI images were produced for each test image using the original MH and ML images (two versions), and using the six fused images. These NDVI images are all high resolution except one of the NDVI image produced from ML. The overall process is illustrated schematically in figure 2.

### 4.1 *Evaluation of data fusion methods*

The average NDVI was computed for each of the 1600 parcels of the base image, for all seven high resolution NDVI images. The NDVI of each parcel obtained from the fused images was compared with the NDVI computed with the original MH data. As an illustration, figure 4 shows a plot of all NDVI values obtained from the Brovey (left) and Wavelet IHS (right) fused data versus NDVI values obtained from the original MH data, for TIS. The plots for the other fusion methods exhibit roughly the same behavior, both for TIS and TIL.

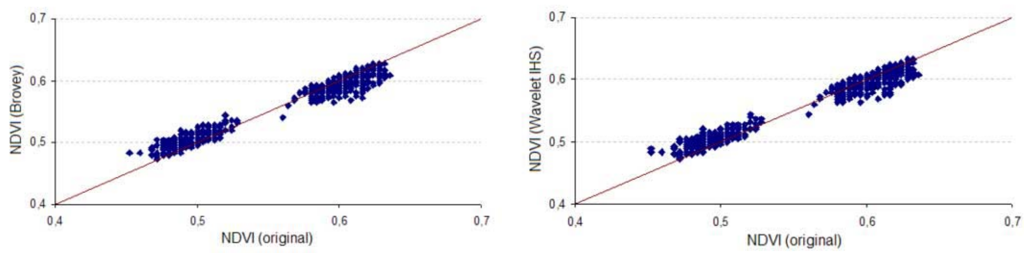


Figure 4. Average NDVI values for all 1600 parcels, computed with Brovey (left) and Wavelet IHS (right) fused data versus the original MH data, for SPOT test image (TIS).

The average absolute errors in NDVI (δ) were computed for all parcels and for all fused images. Average values of δ were calculated for parcels of the same size within each image. These results $(\delta \times 1000)$ are presented in table 1 for the square parcels of TIS. In bold is the best result for each scale tested. Overall the best methods were Brovey, Wavelet IHS and IHS Hexcone, all with low average absolute errors (6.5, 6.7 and 7.2). The values of δ tend to become smaller with the increase of parcel size, as the influence of neighboring parcels becomes less important.

Table 1 – Average absolute error in NDVI (δ x1000) for six data fusion methods for SPOT test image (TIS).

| Parcel size (units) | Brovey | IHS Cylinder | IHS Hexcone | PCA | Wavelet IHS | Wavelet Single Band |
|---|---|---|---|---|---|---|
| 1 | 14.0 | 30.7 | 13.9 | 31.2 | **13.8** | 32.8 |
| 2 | 17.3 | 37.4 | **15.4** | 31.0 | 16.2 | 36.5 |
| 3 | 7.7 | 25.1 | **6.9** | 25.9 | 7.7 | 16.0 |
| 4 | **0.8** | 19.7 | 4.3 | 21.8 | 2.6 | 6.2 |
| 5 | 2.4 | 19.5 | 3.8 | 23.5 | **2.1** | 10.1 |
| 6 | 5.9 | 25.9 | **4.5** | 24.2 | 5.6 | 17.3 |
| 7 | 3.2 | 21.0 | 3.8 | 23.5 | **3.0** | 10.2 |
| 8 | **1.0** | 20.3 | 4.6 | 22.6 | 2.2 | 6.2 |
| All | **6.5** | 25.0 | 7.2 | 25.5 | 6.7 | 16.9 |

A similar experience was carried out with the synthetic data for Landsat (TIL). The results obtained from the fused data are presented in table 2. In bold is the best result for each scale tested. There are four fusion methods that provide NDVI values with low errors (IHS Cylinder, PCA, Wavelet IHS and Wavelet Single Band) while the others two methods (Brovey and IHS Hexcone) do not provide satisfactory NDVI results for all parcel sizes tested.

Table 2 – Average absolute error in NDVI (δ x1000) for six data fusion methods for Landsat test (TIL).

| Parcel size (units) | Brovey | IHS Cylinder | IHS Hexcone | PCA | Wavelet IHS | Wavelet Single Band |
|---|---|---|---|---|---|---|
| 1 | 131.5 | 30.6 | 66.2 | **22.9** | 24.2 | 24.8 |
| 2 | 109.3 | 29.3 | 55.8 | **22.6** | 23.4 | 23.8 |
| 3 | 122.1 | 14.6 | 60.0 | 12.6 | **12.2** | 13.6 |
| 4 | 123.5 | 7.2 | 58.2 | **6.9** | 9.9 | 11.2 |
| 5 | 128.3 | **9.8** | 59.4 | 11.7 | 11.8 | 13.3 |
| 6 | 118.4 | 11.2 | 57.1 | 11.7 | **9.9** | 14.7 |
| 7 | 124.8 | **8.8** | 57.8 | 11.0 | 10.6 | 12.3 |
| 8 | 132.2 | **7.0** | 58.1 | 7.7 | 10.2 | 11.8 |
| All | 123.8 | 14.8 | 59.1 | **13.4** | 14.0 | 15.7 |

An alternative approach is to obtain the NDVI values of each parcel directly from the low resolution multi-spectral image (ML). As the parcels are located in the base image, which is only available in high resolution, this can be achieved by one of two modes: (I) reducing the resolution of the base image, to match the lower resolution multi-spectral image, or (II) increasing the resolution of the ML image to match the resolution of the base image (see figure 2). Each of these modes provides estimates of the NDVI values for each parcel, which can be compared with the reference NDVI obtained directly from the high resolution original test data (MH). The results for TIS and TIL, presented in table 3, are about the same as the best ones from the fused data, with a very slight advantage of mode II. The values of δ are again generally much lower for large parcels.

Table 3 - Average absolute error in NDVI (δ x1000) using the original lower resolution TIS and TIL.

| Parcel size (units) | TIS | | TIL | |
|---|---|---|---|---|
| | Mode I | Mode II | Mode I | Mode II |
| 1 | 13.9 | 13.6 | 28.8 | 21.8 |
| 2 | 19.4 | 17.1 | 26.1 | 22.1 |
| 3 | 6.1 | 7.5 | 7.7 | 9.6 |
| 4 | 0.8 | 0.8 | 5.4 | 5.4 |
| 5 | 2.7 | 2.2 | 10.2 | 8.0 |
| 6 | 6.1 | 5.9 | 9.4 | 8.5 |
| 7 | 3.0 | 2.9 | 5.1 | 6.2 |
| 8 | 1.0 | 1.0 | 5.1 | 5.1 |
| All | 6.6 | 6.4 | 12.2 | 10.8 |

A similar analysis was performed using the evaluation parameters Euclidean Distance (ED), Coefficient of Correlation (R) and Root Mean of Square Error (RMSE) instead of δ. The results obtained for TIS are almost identical to the evaluation based on δ. For TIL, the IHS Cylinder is less rated with these parameters than it was for δ, particularly for R. Otherwise the results for TIL are also consistent with the evaluation based on δ.

## 4.2 *Evaluation of the spatial degradation process*

The image pairs MLGauss / PANGauss and MLGauss / PAN were used to produce two fused images (fusGauss and fusNew), using the IHS Hexcone fusion method. Average values of δ were calculated for parcels of the same size within each image. The results obtained for the two fused images based on MLGauss were compared with those obtained with the fused image obtained directly from ML and PAN, without using a Gaussian filter (FUSED). Figure 5 shows the values of δ for the NDVI images produced from these three fused images, using a range of 0 to 1 (left) and -1 to 1 (right) for the NDVI. The use of a Gaussian filter in the degradation stage results in better NDVI values in the fused images. The range -1 to 1 was found to be better for all methods and scales.

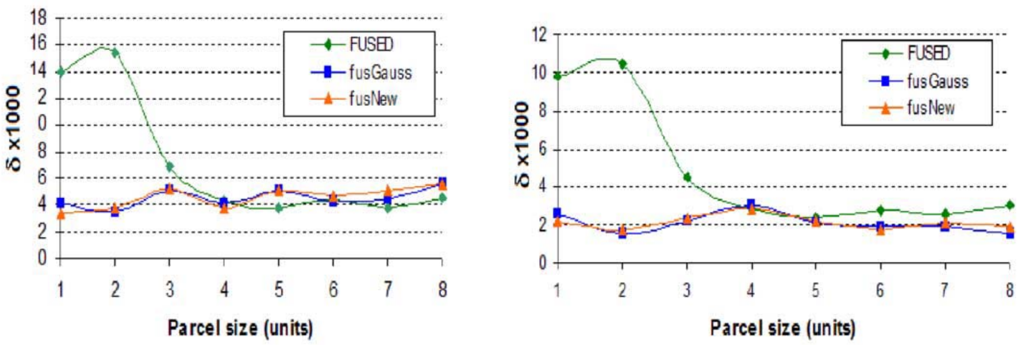


Figure 5: Average absolute error in NDVI (δ x1000) obtained from the fused images with a NDVI range of 0 to 1 (left) and -1 to 1 (right)

## 5 CONCLUSIONS

The methodology proposed, based on the production of synthetic images reproducing real satellite images, proved to be effective for the evaluation of data fusion results. The test images were produced with the Synthetic Image Testing Framework (SITEF), which is available at www.fc.u.pt/sitef. The SITEF software and test datasets can be used to test not only data fusion methods, but also image segmentation and image classification.

The experiment carried out performed an evaluation of six data fusion methods with simulated SPOT HRG and Landsat TM data. For SPOT HRG, the best fusion methods were Brovey, Wavelet IHS and IHS Hexcone, while for Landsat TM the best results were produced from PCA, Wavelet IHS and IHS Cylinder. For the two test datasets combined, the best fusion method was found to be Wavelet IHS. This is in line with the results reported by various authors, such as Vijayaraj *et al* 2004, Karathanassi *et al* 2007 and Zhou *et al* 1998, for pixel and bands based tests. Overall, both the best fusion methods and the lower resolution multi-spectral images produce NDVI average values that are very close to those obtained from the high resolution multi-spectral images (differences in NDVI below 0.02), except for the very small parcels. However, all the evaluation parameters on all images indicate that the smallest error in the computation of NDVI average for land parcels is obtained using the lower spatial resolution multi-spectral image directly, with the parcel location by mode II. This indicates that for quantitative measurements, such as NDVI, there is no benefit from using fused data instead of the original lower resolution multi-spectral data. It is nevertheless worth noting that the best results from the fused data are only marginally worse than those obtained from the lower resolution data.

The evaluation of the spatial degradation process indicates that the use of a Gaussiam filter and the range -1 to 1 for NDVI provides better results when using the fused data to compute average NDVI values per parcel. The spatial degradation mode could be further improved, by using a Modulation Transfer Function filter (Aiazzi *et al* 2006). Other fusion methods, besides the six tested here could perhaps produce better results, such as the modified version of the IHS method proposed by Tu *et al* 2004, and Context-Based Decision which was voted as the best fusion method in a recent contest (Alparone *et al* 2007). However, even with these improvements the best results would still likely be obtained using the low resolution multi-spectral images, as data fusion methods are not intended to improve spectral information but rather the visual interpretation.

## ACKNOWLEDGMENTS

This work is part of the FCT LameSat_XXI project (PTDC/AGR-AAM/67182/2006). The authors wish to thank the OASIS programme (nº307) for providing the SPOT satellite image, and Isabel Pôças for the identification of land cover types.

## REFERENCES

Aiazzi, B., Alparone, L., Baronti, S., Garzelli, A. & Selva, M. 2006. *MTF-tailored multiscale fusion of high-resolution MS and Pan imagery*. Photogrammetric Engineering and Remote Sensing, vol.72, no.5, 591-596.

Alparone, L., Wald, L., Chanussot, J., Thomas, C., Gamba, P. & Bruce, L. 2007. *Comparison of Pansharpening Alghorithms: Outcome of the GRS_S Data Fusion Contest.* IEEE Transactions on Geoscience and Remote Sensing, vol.45, no.10.

Balcik, F.B. & Sertel, E. 2007. *Wavelet_Based Image Fusion of Landsat ETM Images: A Case Study for Different Landscape Categories of Istanbul* (Presented Conference Paper style). Conference on Information Extraction from SAR and Optical Data, with Emphasis on Developing Countries. Istanbul 2007.

Erdas Imagine. 2007. http://gi.leica-geosystems.com/default.aspx . Consulted in 2007-12-19.

FIFE. 2004. *http://dac.ornl.gov/FIFE/guides/Satellite_SPOT_Extracted_Data.html#4.1. Satellite SPOT Extracted Data.* Consulted in 2007-12-12.

GAEL 2003. http://earth.esa.int/pub/ESA_DOC/landsat_FAQ/. *Inventory of Landsat product anomalies*, Issue 1, Revision 0, 5-11. Consulted in 2007-11-07.

Jensen, J.R., 2000. *Remote Sensing of The Environment – An Earth Resource Perspective*. Prentice Hall.

Karathanassi, V., Kolokousis, P. & Ioannidou, S. 2007. A *comparison study on fusion methods using evaluation indicators*. International Journal of Remote Sensing, vol. 28, no. 10, 2309-2341.

Marçal, A.R.S. & Rodrigues, A.S. 2008. *A Framework for the Evaluation of Multi-Spectral Image Segmentation.* Submitted to the Proceedings of GEOBIA 2008, August 2008, Calgary, Canada.

Meenakshisundaram, V. & Couloigner, I. 2005. *Quality assessment of Fusion Methods for High Resolution Images*. 3rd International Symposium Remote Sensing and Data Fusion Over Urban Areas. USA 2005.

PCI Geomatics. 2005. http://www.pcigeomatics.com/ .Consulted in 2007-12-19.

Ranchin, T. & Wald, L. 2000. *Fusion of High Spatial and Spectral Resolution Images: The ARSIS Concept and its Implementation*. Photogrammetric Engineering & Remote Sensing, vol. 66, no.1, 49–61.

Scheunders, P. & Backer, S.De. 2001. *Fusion and merging of multispectral images using multiscale fundamental forms*. Journal of the Optical Society of America A, vol.18, no.10, 2468-2477.

Tu, T.M., Huang, P.S., Hung, C.L. & Chang, C.P. 2004. *A Fast Intensity-Hue-Saturation fusion technique with spectral adiustment for IKONOS imagery*. IEEE Geoscience and Remote Sensing Letters, vol.1, no.4, 309-312.

Vijayaraj, V., O'Hara, C. G. & Younan, N. 2004. *Quality analysis of Pansharpened Images*. Geoscience and Remote Sensing Symposium. IEEE International, vol.1, 85- 88.

Wald, L. 2002. *Data Fusion: Definitions and Architectures – Fusion of images of different spatial resolutions*. Paris: Les Presses de l´École des Mines.

Wang, L., Zhang, Y. & Feng, J. 2005a. *On the Euclidian Distance of Images*. IEEE Transactions on Pattern Analysis and Machine Intelligence, vol.27, no.8, 1334- 1339.

Wang, Z., Ziou, D., Armenakis, C., Li, D. & Li, Q. 2005b. *A Comparative Analysis of Image Fusion Methods*. IEEE Transactions on Geoscience and Remote Sensing, vol. 43, no.6, 1391-1402.

Wehrmann, T., Colditz, R.R., Bachmann, M., Steinnocher, K. & Dech, S. 2005. *Evaluation of Image Fusion Techniques*. Remote Sensing & GIS Environmental Studies, vol.113, 296-302.

Zhou, J., Civco, D.L. & Silander, J.A. 1998, *A wavelet transform method to merge Landsat TM and SPOT panchromatic data*. International Journal of Remote Sensing, vol. 19, no. 4, 743-757.